Structural visualization of two electric field regimes of polarization fatigue in epitaxial ferroelectric oxide devices

Dal-Hyun Do[1], Paul G. Evans[1], Eric D. Isaacs[2], Dong Min Kim[1], Chang Beom Eom[1], and Eric M. Dufresne[3]

[1] Department of Materials Science and Engineering, U. of Wisconsin, Madison, WI 53706

[2] Bell Laboratories, Lucent Technologies, Murray Hill, NJ 07974; Presently at Center for Nanoscale Materials, Argonne National Laboratory, Argonne, IL 60439.

[‡] Department of Physics, U. of Michigan, Ann Arbor MI 48109

Correspondance should be addressed to PE.

Ferroelectric oxides, such as $Pb(Zr,Ti)O_3$, have tremendous potential for electronic and photonic devices because of their ability to retain two stable polarization states which can form the basis for memory and logic circuitry. Requirements for long-term operation of practical devices such as non-volatile RAM include consistent polarization switching over many (more than 10^{12}) cycles of the applied electric field, which represents a major challenge. A primary limitation common to all practical devices is so-called polarization fatigue, the reduction in the amount of switchable polarization after a large number of switching cycles. Since switching is largely controlled by the motion and pinning of domain walls, it is essential to develop suitable tools that can directly probe the ferroelectric domain structures in operating devices, i.e., thin film structures with electrical contacts. The recently

developed technique of synchrotron x-ray microdiffraction complements existing microscopic probes and allows us to visualize the evolution of polarization domains in ferroelectric devices directly, through metal or oxide electrodes, and with sub-micron spatial resolution. The images reveal two unique regimes of fatigue depending on the magnitude of the electric field pulses driving the device: a low-field regime in which fatigue can be reversed with higher electric field pulses, and a high-field regime in which there is a non-reversible crystallographic relaxation of the epitaxial ferroelectric film.

A common feature of ferroelectric capacitors (e.g. as in Figure 1a) is a rapid decrease in the polarization that can be switched following many cycles of an applied electric field.[1] This polarization fatigue has been attributed to several causes that depend in detail on the structure of the device. In devices with elemental metal electrodes, fatigue has been linked to the migration of oxygen to the electrode-ferroelectric interface and the development of oxygen vacancy clusters which can inhibit the switching by pinning domain walls.[2] A second possibility involves the formation of layers at electrode interfaces that effectively reduce the total electric field applied across the device or inhibit the nucleation of oppositely polarized domains.[3, 4] These mechanisms modify the dynamics of ferroelectric domains in applied electric fields and depend on the magnitude and frequency of the field as well as the details of the device preparation. The candidate mechanisms for polarization fatigue have been identified in area-integrated electrical measurements.[4] Microscopy, however, has shown that both polarization switching[5] and the eventual evolution of fatigue in operating devices is inhomogeneous on the micron

scale.[6] Structural measurements have thus far been limited to either much larger scales or, using transmission electron microscopy, to unfavorable sample geometries that complicate *in situ* observations during device operation. In comparison with techniques such as measurements of the piezoelectric response of the ferroelectric material with an atomic force microscope,[7] x-ray microdiffraction is a structural probe that does not require an electric field be applied during imaging and is not complicated by the mechanical properties of the sample[8].

$PbZr_{1-x}Ti_xO_3$ (PZT) is considered one of the most attractive materials for ferroelectric devices because it has a large polarization, has the simple ABO_3 perovskite structure, and is reasonably straightforward to synthesize. For this study, prior to PZT films, epitaxial $SrRuO_3$ (SRO) bottom electrodes were deposited on single crystal (001) SrTiO3 substrates by off-axis radio-frequency (RF) magnetron sputtering.[9] The epitaxial PZT films were grown on these electodes by on-axis RF magnetron sputtering . The nominal composition of the films, x=0.55, was chosen to be on the tetragonal side of the morphotropic phase boundary separating tetragonal and rhombohedral structural phases of PZT.[10] Polycrystalline platinum thin film top electrodes were deposited by magnetron sputtering through a shadow mask defining 200 μm diameter capacitor devices.

We have used x-ray microdiffraction,[11] a novel spatially resolved technique for probing ferroelectrics, to differentiate between two regimes of electric field amplitude in the development of fatigue in epitaxially grown ferroelectric devices. In order to resolve the microscopic processes involved in the switching and fatigue of ferroelectric devices, we have used synchrotron x-ray microdiffraction based on Fresnel zone plate focusing

optics, which provide the smallest spot size for hard x-rays.[12] A 10 keV x-ray beam from the 7ID beamline of the Advanced Photon Source was focused to an 800 nm spot and easily penetrated the top electrode (Figure 1b), allowing electrical measurements to be carried out *in situ* without removing the sample from the diffractometer. The x-ray penetration length is on the order of several microns or more in the materials from which our sample is made and thus our measurements effectively average through the depth of the film. Microdiffraction provides information on the bulk of the thin film.Images of the polarization within ferroelectric devices were formed by scanning the sample in the focused beam and continuously monitoring the intensity of the PZT c-axis Bragg reflections. Upon polarization reversal we observed a 30% change in the intensity of PZT reflections, which formed the basis for our image contrast. The change in intensity is a crystallographic effect that is connected to the change in the index of the surface-normal c-axis x-ray reflection (for example from 002 to 002) that occurs during switching. Friedel's law ordinarily requires that intensities at reciprocal space points related by inversion (e.g. *hkl* and $\bar{h}\bar{k}\bar{l}$) be equal, but does not apply in cases in which absorption is important.[13] This approach using the intensity of x-ray reflections to distinguish oppositely polarized regions of ferroelectrics has been widely used in the study of ferroelectric domains in bulk crystals of lithium niobate with x-ray topography, as well as in the determination of the absolute orientation of other materials with polar unit cells.[14,16]

Images of a PZT device in the remnant polarization state, at zero applied voltage after the application of a voltage pulse, were taken for both stable polarization states. We first

established that x-ray microdiffraction was an accurate probe of the local stored ferroelectric polarization. By applying voltage pulses to the bottom electrode, the PZT thin film was switched between stored polarization states in which the [001] and $[00\bar{1}]$ directions were normal to the device surface. Images of a region including the edge of an electrode (Figure 1c) show the effect of switching the remnant polarization on the intensity of the x-ray reflection from the film. Each image required approximately 30 min to acquire. No evolution of images with time was observed in repeated scans of the same area.[17] The mean intensity of the reflection from the device area is 30% greater following a -1.25 MV cm^{-1} 500 μs-duration triangular electric field pulse to the bottom electrode than for an identical positive pulse. By following -1.25 MV cm^{-1} pulses with positive voltage pulses of amplitudes near the coercive field, we found that the polarization was switched in discrete areas of the film and that the switched area in the x-ray microdiffraction images was proportional to the net reversal of the stored polarization (Figure 1d). Aside from the overall change in intensity, rocking curves and theta-two theta scans showed no difference between the two polarization states. There was no change in the intensity of the (002) reflection in the area of the PZT film not covered by the top electrode.

The development of polarization fatigue resulted in the collapse of the polarization-electric field hysteresis loops upon repeated cycling of the applied electric field. Using 1 kHz triangle wave fields, we found that after a number of cycles the switchable polarization rapidly decreased from an initial value of 95 μC cm^{-2} (Figure 2a). The onset of fatigue occurred in two qualitative regimes. At pulse amplitudes of 10 V applied to

the 160 nm-thick PZT films (a nominal field of 625 kV cm^{-1}) we found fatigue within 10^4 cycles and an eventual decrease of the switchable polarization to 25 μC cm^{-2} (Figure 2b). We used the same pulse waveforms for both hysteresis loop and fatigue measurements to avoid complications caused in measurements with insufficient electric field or pulse duration.[18] Microdiffraction maps of the rapid fatigue process in this low electric field regime show that as a result of fatigue the PZT layer gradually becomes pinned in the state that would normally be reached by applying a positive voltage to the bottom electrode. Figure 3a shows the evolution of the intensity of the x-ray reflections in pairs of images taken following positive and negative voltage pulses at interruptions in cycling the electric field after increasing numbers of cycles. The difference in the integrated intensity between pairs of images is a measure of the switching of the polarization.

The low-field fatigue process preserves the crystal structure of the PZT layer, but pins it in a state in which it can no longer respond to applied voltage pulses. Larger amplitude voltage pulses (up to ±19 V, 1.2 MV cm^{-1}) restored the switchable polarization observable both in x-ray images and electrical measurements (Figure 3b). It has been observed previously that larger fields may be sufficient to allow the nucleation of domains or to de-pin domain walls when switching at lower voltages is suppressed.[4,19,20]

The composition of the metal electrodes can have an important role in the onset of fatigue. It has been often observed that fatigue is delayed in devices using complex oxide metal electrodes.[21] In previous studies, SRO top electrode layers have delayed the onset of fatigue to the order of 10^{10} or more cycles.[22] We found that the low-field mechanism of fatigue was not observed in up to 5×10^7 electric field cycles in devices fabricated

using SRO rather than Pt top electrodes, suggesting a chemical driving force for low-field fatigue, such as the oxygen vacancy mechanism proposed previously by Dawber *et al*.[2] The development of fatigue and the clear preference for a single polarization state suggest that the asymmetry of the electrode composition (i.e. epitaxial SRO bottom electrodes vs. Pt top electrodes) is important. However, we observed only a slight shift in the coercive field (by –0.2 V, or 12.5 kV cm^{-1}) during the fatigue process indicating that the applied fields were well above the effective coercive fields and that low-field fatigue originated in either pinning of domain motion or the effective suppression of nucleation.[4] In addition, hysteresis loops retained a sharp transition at the coercive field throughout the fatigue process. The fatigue mechanism is thus not simply due to a gradual development of imprint in local areas of the film.

The origin of polarization fatigue is dramatically different in measurements made at higher electric fields. With pulse amplitudes of 1.2 MV cm^{-1}, resulting from 19 V pulses applied to a 160 nm film or 10V across an 80 nm film, the onset of fatigue occurred after 2×10^5 or more cycles of the field (Figure 2b) a factor of approximately 10^2 more than at lower fields. Fatigue at high electric field, however, was accompanied by a much larger eventual decrease in the switchable polarization and no rejuvenation with higher fields was possible. The eventual decrease of switchable polarization is accompanied by a dramatic structural change in the PZT thin film. For a small number of cycles, the result of switching at high fields is similar to what is observed at low fields; the PZT film switches uniformly between polarization states. As fatigue develops in the high field case, however, the x-ray reflections in some areas of the film decrease in intensity by up

to a factor of ten. These regions, which are at first isolated, coalesce at larger numbers of polarization cycles and eventually cover the entire area beneath the electrodes (Figure 4). The fraction of the area of the device occupied by these regions of drastically reduced intensity increases as fatigue develops and scales with the decrease in the switchable polarization (Figure 2b). In the areas of the film initially unaffected by fatigue there was no reduction in the intensity difference between states prepared by positive and negative pulses. The failure of devices fabricated from 160 nm PZT layers in the high electric field regime was more dramatic, resulting in damage to the device that was visible under an optical microscope. High-field fatigue was distinct from the process of catastrophic shorting of these devices, which occurred at still higher electric fields.

The structural effect of polarization fatigue at high electric fields is clear in reciprocal space as well. We have already noted the factor-of-ten decrease in the intensity of reflections at the as-grown lattice spacing of the PZT film. In addition, following high-field fatigue, the PZT (002) reflection is broader in reciprocal space scans along [00L] and in rocking curve measurements. For the thinner films, which are under strain following growth, the peak intensity of the PZT reflection is shifted during the high-field fatigue process to higher 2θ angle, corresponding to a 0.3% decrease in the PZT out-of-plane lattice constant (Figure 4b) and a shift towards the bulk lattice parameter. The thicker, 160 nm films were fully relaxed before fatigue and exhibited the decrease in intensity, but only a slight shift in the reciprocal space position of the (002) reflection. The structural changes may be related to the formation of defects relaxing the epitaxial strain or to the accumulation of oxygen vacancies in increasingly thick regions near the Pt

electrode.[23] Because our sampling of the diffraction pattern was limited to the vicinity of a single point in reciprocal space, the subtle structural changes with low field fatigue as observed by Thompson *et al*. [24] in an x-ray crystal truncation rod measurement cannot be ruled out.

These x-ray microdiffraction measurements confirm previous suggestions that there are several important mechanisms of fatigue and show that multiple mechanisms can simultaneously be important to an individual device. Recently, area-averaged dielectric loss measurements have also suggested that multiple mechanisms can be at work simultaneously.[25] In our case, at low fields the development of a single polarization state without a general shift in the coercive electric suggests that the nucleation and growth of domains of the opposite polarization is suppressed. If domain wall pinning is the origin of this fatigue process, the motion of domain walls is ultimately hindered at scales smaller than our x-ray spot size. At high fields, the fatigue process is irreversible and results in a drastic reduction of structural order in the PZT film. The structural understanding and control of fatigue presents an important continuing challenge to the realization of microelectronic and photonic devices based on ferroelectric oxide materials. X-ray microdiffraction is the ideal tool for understanding these and other complex materials in which structural, electronic and even magnetic phenomena are deeply intertwined.

Acknowledgement

This work was supported by the National Science Foundation through the University of Wisconsin Materials Research Science and Engineering Center, grant no. DMR-

0079983 and by under grant no. DMR-0313764 (CBE). Use of the Advanced Photon Source was supported by the U. S. Department of Energy, Office of Science, Office of Basic Energy Sciences, under contract no. W-31-109-Eng-38. ED acknowledges support from the U.S. Department of Energy, grants no. DE-FG02-03ER46023 and DE-FG02-00ER15031, and from the NSF FOCUS physics frontier center.

References

[1] J. F. Scott, *Ferroelectric Memories*, Springer, Berlin (2000).

[2] M. Dawber and J. F. Scott, A model for fatigue in ferroelectric perovskite thin films. Appl. Phys. Lett. **76**, 1060 (2000).

[3] P. K. Larsen, G. J. M. Dormans, D. J. Taylor, and P. J. van Veldhoven, Ferroelectric properties and fatigue of $PbZr_{0.51}Ti_{0.49}O_3$ thin films of varying thickness: Blocking layer model. J. Appl. Phys. **76**, 2405 (1994).

[4] A. K. Tagantsev, I. Stolichnov, E. L. Colla, and N. Setter, Polarization fatigue in ferroelectric films: Basic experimental findings, phenomenological scenarios, and microscopic features. J. Appl. Phys. **90**, 1387 (2001).

[5] V. Nagarajan, A. Roytburd, A. Stanishevsky, S. Prasertchoung, T. Zhao, L. Chen, J. Melngailis, O. Auciello, and R. Ramesh, Dynamics of ferroelastic domains in ferroelectric thin films. Nature Materials, **2**, 43 (2002).

[6] E. L. Colla, S. Hong, D. V. Taylor, A. K. Tagantsev, N. Setter, and K. No, Direct observation of region by region suppression of the switchable polarization (fatigue) in Pb(Zr, Ti)O_3 thin film capacitors with Pt electrodes. Appl. Phys. Lett. **72**, 2763-2765 (1998).

[7] A. Gruverman, O. Auciello, and H. Tokumoto, Imaging and control of domain structures in ferrolectric thin films via scanning force microsopy. Ann. Rev. Mat. Sci. **28**, 101-123 (1998).

[8] R. C. Rogan, N. Tamura, G. A. Swift, and E. Üstündag, Direct measurement of triaxial strain fields around ferroelectric domains using X-ray microdiffraction. Nature Materials **2**, 379 (2003).

[9] C. B. Eom, R. J. Cava, R. M. Fleming, J. M. Phillips, R. B. van Dover, J. H. Marshall, J. W. P. Hsu, J. J. Krajewski, W. F. Peck, Jr., Single-crystal epitaxial thin films of the isotropic metallic oxides $Sr_{1-x}Ca_xRuO_3$ ($0 \leq x \leq 1$). Science **258**, 1766-1769 (1992).

[10] B. Noheda, D. E. Cox, G. Shirane, J. A. Gonzalo, L. E. Cross and S-E. Park, A monoclinic ferroelectric phase in the $Pb(Zr_{1-x}Ti_x)O3$ solid solution. Appl. Phys. Lett. **74**, 2059-2061 (1999).

[11] Z. Cai, B. Lai, Y. Xiao, and S. Xu, An X-ray diffraction microscope at the Advanced Photon Source. J. de Physique IV **104**, 17-20 (2003).

[12] B. Lai, W. B. Yun, D. Legnini, Y. Xiao, J. Chrzas, P. J. Viccaro, V. White, S. Bajikar, D. Denton, F. Cerrina, E. Di Fabrizio, M. Gentili, L. Grella, and M. Baciocchi, Hard x-ray phase zone plate fabricated by lithographic techniques. Appl. Phys. Lett. **61**, 1877-1879 (1992).

[13] R. W. James, *The Optical Principles of X-ray Diffraction*, Ithaca, N. Y., Cornell University Press (1965), p. 33.

[14] C. A. Wallace, The display of twinning in lithium niobate by x-ray diffraction topography. J. Appl. Cryst. **3** 546 (1970).

[15] T. Vreeland and V. S. Speriousu, Defects and domains in $LiNbO_3$. in *Applications of X-ray Topographic Methods to Materials Science*, F. Balibar and J.-F. Petroff, eds., Plenum Press, New York (1984), pp. 501-509.

[16] D. Coster, K. S. Knol, and J. A. Prins, Difference in the intensities of x-ray reflection from the two sides of the 111 plane of zinc blende, Z. Phys. **63** 345-369 (1930).

[17] Long-term exposure to the beam, with total incident flux on the order of 10^{12} to 10^{13} photons μm^{-2}, caused permanent beam damage to the PZT film.

[18] M. Grossmann, D. Bolten, O. Lohse, U. Boettger, R. Waser, and S. Tiedke, Correlation between switching and fatigue in $PbZr_{0.3}Ti_{0.7}O_3$ thin films. Appl. Phys. Lett. **77**, 1894-1896 (2000).

[19] E. L. Colla, A. K. Tagantsev, D. V. Taylor and A. L. Kholkin, Fatigued state of the Pt-PZT-Pt system. Integrated Ferroelectrics **18**, 19-28 (1997).

[20] J. F. Scott and B. J. Pouligny, Raman spectroscopy of submicron KNO3 films. II. Fatigue and space-charge effects. J. Appl. Phys. **64**, 1547-1561 (1988).

[21] O. Auciello, K. D. Gifford, D. J. Lictenwalner, R. Dat, H. N. Al-Shareef, K. R. Bellur, and A. I. Kingon, Review of composition-structure-property relationships for PZT-based heterostructure capacitors. Integrated Ferroelectrics **6**, 173-187 (1995).

[22] C. B. Eom, R. B. Van Dover, J. M. Phillips, D. J. Werder, J. H. Marshall, C. H. Chen, R. J. Cava, R. M. Fleming, and D. K. Fork, Fabrication and properties of epitaxial ferroelectric heterostructures with ($SrRuO_3$) isotropic metallic oxide electrodes. Appl. Phys. Lett. **63**, 2570-2572 (1993).

[23] H. M. Duiker, P. D. Beale, J. F. Scott, C. A. Paz de Araujo, B. M. Melnick, J. D. Cuchiaro, and L. D. McMillan, Fatigue and switching in ferroelectric memories: theory and experiment. J. Appl. Phys. **68** 5783-5791 (1990).

[24] C. Thompson, A. Monkholm, S. K. Streiffer, G. B. Stephenson, K. Ghosh, J. A. Eastman, O. Auciello, and G.-R. Bai, M. K. Lee, and C. B. Eom, X-ray scattering evidence for the structural nature of fatigue in epitaxial Pb(Zr, Ti)O_3 films. Appl. Phys. Lett. **78**, 3511-3513 (2001).

[25] A. Jiang, M. Dawber, J. F. Scott, C. Wang, P. Migliorato, and M. Greg, Japan. J. Appl. Phys. **42** 6973-6982 (2003).

Figure 1: Polarization switching in a PZT thin film capacitor a, Epitaxial ferroelectric capacitor fabricated on an (001) oriented $SrTiO_3$ substrate. **b,** A schematic of the synchrotron x-ray microdiffraction experiment. **c,** Images of the intensity of a the (002) reflection of $Pb(Zr,Ti)O_3$ following -10 V and +10 V pulses to the bottom electrode of the capacitor device. The intensity of the reflection varies with local ferroelectric polarization and changes by 30% upon polarization switching. **d,** The area of the region in which the intensity has changed (triangles) and the total switched polarization (solid line) are proportional and provide independent observations of the switching process.

Figure 2: Polarization fatigue a, Polarization-electric field hysteresis loops for the 160 nm PZT thin film exhibit polarization fatigue after approximately 10^4 electric field cycles. **b,** When operated at the same voltage, capacitors fabricated from 80 nm thin films (squares) required a factor of roughly 10^2 more cycles to be fatigued to the same remnant polarization as those fabricated from 160 nm PZT layers. The evolution area of regions of reduced (002) reflection intensity measured from the images of Fig. 4 is consistent with the decrease in switchable polarization.

Figure 3: Low field fatigue a, Images of the evolution of the intensity of the PZT (002) reflection during fatigue under low electric field conditions. The film is eventually pinned in the state that would normally follow a positive voltage pulse to the bottom electrode. **b,** An electric field pulse of a larger magnitude restores the switchable polarization.

Figure 4: High field fatigue a, The evolution of polarization fatigue under high fields occurs by the development and spread of areas of reduced x-ray reflection intensity. **b,**

The PZT (002) reflection is shifted to smaller lattice constant in these areas, consistent with the relaxation of the strain resulting from epitaxial growth.

A

Pt or $SrRuO_3$ top electrode

epitaxial $Pb(Zr,Ti)O_3$ ferroelectric thin film

$SrRuO_3$ bottom electrode

$SrTiO_3$ (001) substrate

B

area of images

focused incident x-ray beam

200 µm dia. electrode

diffracted beam to detector

[001]

C

-10 V

+10 V

20 µm

0

1

intensity

D

ΔP_r for +10V pulse

ΔP_r ($\mu C\ cm^{-2}$)

switched area fraction

pulse amplitude (V)

0 20 40 60 80 100

0 0.2 0.4 0.6 0.8 1

0 0.5 1 1.5 2 2.5

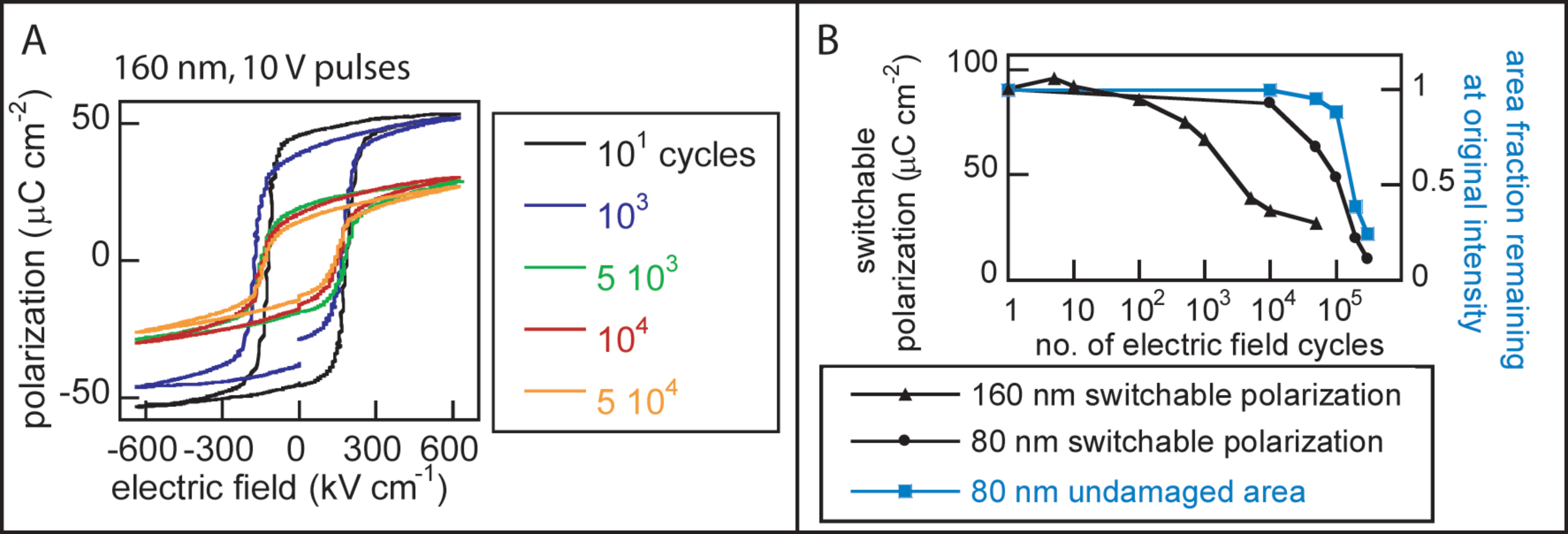
A
160 nm, 10 V pulses
polarization (μC cm-2)
50
0
-50
-600 -300 0 300 600
electric field (kV cm-1)
10^1 cycles
10^3
5 10^3
10^4
5 10^4
B
switchable polarization (μC cm-2)
100
50
0
1 10 10^2 10^3 10^4 10^5
no. of electric field cycles
1
0.5
0
area fraction remaining at original intensity
160 nm switchable polarization
80 nm switchable polarization
80 nm undamaged area

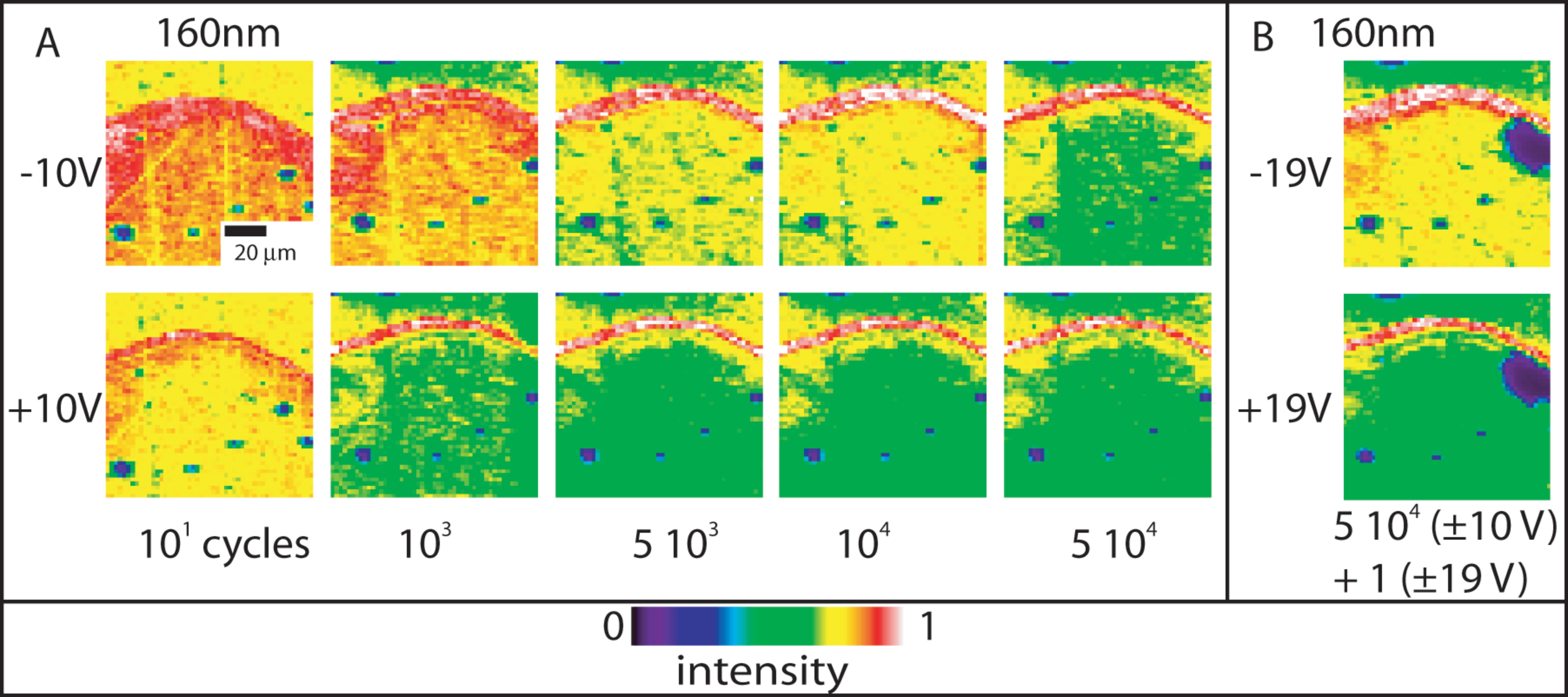
A
160nm
-10V
+10V
20 µm
10^1 cycles
10^3
5 10^3
10^4
5 10^4
B
160nm
-19V
+19V
5 10^4 (±10 V)
+ 1 (±19 V)
0
1
intensity

A 80nm

-10V

+10V

20 µm

1

intensity

0

10^1 cycles $5\ 10^4$ 10^5 $2\ 10^5$ $3\ 10^5$

B